Terahertz-Wave Generation Based on Optical Frequency Comb and Single Mach-Zehnder Modulator
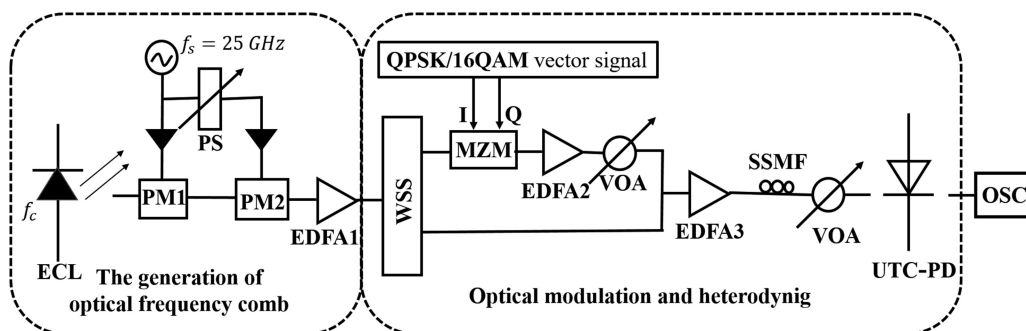
Jianguo Yu
Kaile Li
Yuanxiang Chen
Lun Zhao
Yongtao Huang
Yitong Li
Jie Ma
Feilong Shan

Terahertz-Wave Generation Based on Optical Frequency Comb and Single Mach-Zehnder Modulator

Jianguo Yu,[1] **Kaile Li,**[1] **Yuanxiang Chen,**[1] **Lun Zhao,**[2]
Yongtao Huang,[1] **Yitong Li,**[1] **Jie Ma,**[1] **and Feilong Shan**[1]

[1]School of Electrical Engineering, Beijing University of Posts and Telecommunications, Beijing, China
[2]Lab of Ubiquitous Wireless Communication Technology, Chongqing University of Posts and Telecommunications, Chongqing, China

Abstract: A novel Terahertz-wave (THz-wave) generation on the strength of optical frequency comb and single push-pull Mach-Zehnder modulator (MZM) with a pair of transmitter and receiver in 0.4-THz band is proposed. The advantages of the optical frequency comb based on phase modulator (PM) 1 and PM2 in series includes the uncomplicated operation and good stability to produce numerous subcarriers at 25-GHz intervals. THz-wave is generated based on two comb lines derived from the same optical frequency comb. One comb line is used as an optical local oscillator (LO) and the other is served as signal carrier for data modulation for heterodyne mixing. We investigate the generation and transmission of a 0.4 THz THz-wave signal carrying 4 Gbaud quadrature-phase-shift-keying (QPSK) or 1 Gbaud 16 quadrature amplitude modulation (16-QAM) data over back-to-back (BTB) transmission or 10 km standard single-mode fiber (SSMF) transmission, with the bit-error-rate (BER) performance below the hard decision forward error correction (HD-FEC) threshold of 3.8e-3.

Index Terms: THz-wave generation, optical frequency comb, QPSK modulation, 16-QAM modulation, UTC-PD.

1. Introduction

With the rapid expansion of the wireline and wireless communication in the last few decades, the photonic-assisted THz-wave (0.3 THz–10 THz) is gradually becoming a potential choice to supply large bandwidth and long-distance high-capacity services to meet the urgent requirements [1]–[4]. This enables wireless communication in the THz-band to offer several gigabits or even hundreds of gigahertz of mobile data transmission per second on account of its inherently wider bandwidth [5]–[12]. However, the higher the frequency would result in a larger transmission loss of the signals, which has a great influence on the transmission distance of the THz-wave signal. Meanwhile, optical radio over fiber (RoF) on the strength of THz-wave has emerged in the last few years. Therefore, it's well worth investigating the vector THz-wave generation techniques in the RoF system.

There are many ways to generate photonic THz-wave signal, which can be mainly divided into three categories. The first category is on the strength of the directly modulated laser (DML) to convert electrical signals into optical signals, which has an uncomplicated and economical architecture. At the transmitting terminal, they apply photonics assisted method to generate THz-wave signal. At the receiving terminal, they down convert the signal to intermediate frequency of around or tens of gigahertz. Then the down-converted signals are applied to drive the directly modulated laser (DML) or intensity modulator to realize electrical-to-optical conversion. The converted optical signals can be transmitted to longer distance in optical fiber. Compared with the electrical absorption modulator (EAM) or intensity modulator such as MZM, DML has a smaller size and uncomplicated structure. However, it's easily limited by the modulation rate and bandwidth of the laser [13], [14]. The second category is optical heterodyne beat scheme. In the remote heterodyne technique, two light carriers of different wavelengths generated from two separate lasers, and the fixed THz-wave can be obtained after passing through the beat frequency of the optical detector and the high speed baseband signal can be transparently loaded onto the THz-wave carrier [4]–[9], [15]–[20]. But it is based on multiple free running lasers, the frequency interval of lasers and their phases float on their own, phase noise regulation procedure at receiver end is required to be processed in DSP, which contributes to the increase of the processing time and system complexity [21]. The third category is the optical frequency comb based on only single laser and optical modulators in series in the THz-band RoF systems [11], [15], [18], [22]–[24]. This breakthrough is produced by a combination of electronics and terahertz photonics, which produces a narrow-band terahertz carrier by mixing the comb-shaped lines of the mode-locked laser in uni-traveling carrier photodiode (UTC-PD) [25], [26]. Therefore, the optical frequency comb on account of single laser and optical modulators in series avoids the phase noise derived from two free-running lasers perfectly. Lately, a few investigators have utilized the optical frequency comb on the strength of only single laser and cascaded optical modulators with single in-phase/quadrature (IQ) modulator in the THz-band RoF system. However, the last category has a quite complicated architecture. Compared to the single drive electro-optic intensity modulator (IM) and PM, IQ modulator is more expensive and more complicated [27]. Besides, it requires three direct current bias settings, which makes the system complex and difficult to adjust [27].

In this paper, a novel Terahertz-wave (THz-wave) generation on the strength of optical frequency comb band and single push-pull MZM in 0.4-THz band is proposed. The optical frequency comb based on PM1 and PM2 in series has obvious advantages including the uncomplicated operation and good stability to produce numerous subcarriers at 25-GHz intervals. The THz-wave signal based on an optical tone and single optical local oscillator selected from the optical frequency comb is generate in a UTC-PD. We investigate the generation and transmission of a 0.4 THz THz-wave signal carrying 4 Gbaud QPSK and 1 Gbaud 16-QAM data over back-to-back transmission or 10 km SSMF transmission, with the BER performance below the HD-FEC threshold of 3.8e-3. To our knowledge, there are few works on the generation of the THz-wave based on optical frequency comb and single push-pull MZM before.

2. Principle

Fig. 1 shows the principle of the proposed generation of the THz-wave signal. The continuous-wave (CW) lightwave located at the frequency f_c derived from one narrow linewidth laser is applied to generate the optical frequency comb in cascaded PMs. Here, the CW lightwave is given by

$$E_{cw}(t) = E_0 \exp(j2\pi f_c t) \tag{1}$$

where E_0 represents the amplitude of the CW lightwave and is constant. The PMs applied here have the same half-wave voltage V_π, then transformation equation of phase modulator (PM) can be given by

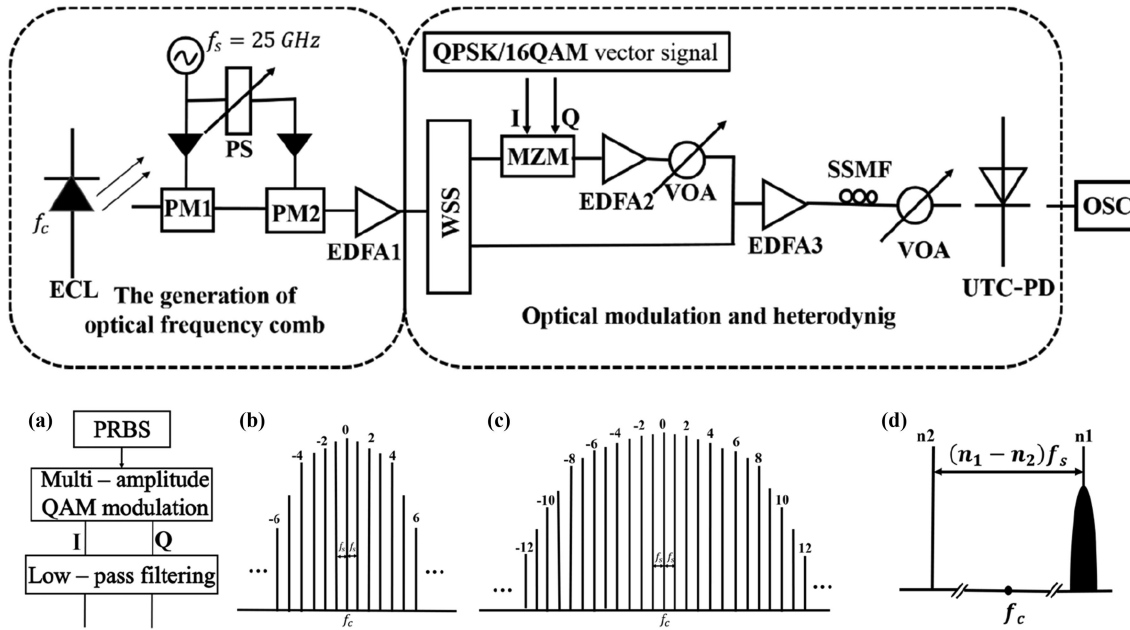$$E_{PM}(t) = E_{cw} \exp\left(j\pi \frac{V_d}{V_\pi}\right) \tag{2}$$

Fig. 1. Concept of the proposed generation of the THZ-wave signal on the strength of optical frequency comb and single push-pull MZM. ECL: external cavity laser; PS: phase shifter; PM: phase modulator; EDFA: erbium doped optical fiber amplifier; WSS: Wavelength selector switch; VOA: variable optical attenuator; SSMF: standard single-mode fiber; OSC: oscilloscope. (a) Vector-modulated QPSK/16QAM signal generation. (b) Output spectra of PM1. (c) Output spectra of PM2. (d) The optical spectrum before UTC-PD.

where V_d denotes the drive signal. Due to the input optical signal of PM1 is $E_{cw}(t)$, the radio frequency (RF) drive signal is given by

$$V_d(t) = RV_\pi \sin(2\pi f_s t) \qquad (3)$$

where R denotes the ratio of RF drive signal voltage to the V_π, f_s is the frequency of the actuating RF signal. Therefore, the output lightwave of PM1 is given by

$$E_{PM1}(t) = E_{cw} \exp[j\pi R_1 \sin(2\pi f_s)]$$

$$= E_0 \exp(j2\pi f_c t) \exp(j\pi R_1 \sin 2\pi f_s t)$$

$$= E_0 \sum_{n=-\infty}^{+\infty} J_n(\pi R_1) \exp[j2\pi(f_c + nf_s)] \qquad (4)$$

where J_n is the first kind and order n Bessel function and $J_{-n}(\pi R) = (-1)^n J_n(\pi R)$. From Eq. (4), the output optical signal consists of one optical central carrier and serval subcarriers at the frequency of $f_c + nf_s$, where $n = \pm 1, \pm 2, \pm 3 \ldots$, as shown in Fig. 1(b). According to the first kind Bessel function, the power of the nth subcarrier is $E_0|J_n(\pi R)|^2$.

Generally speaking, the power of the high-order subcarriers and the amount of the subcarriers will increase by R [24]. Because of the limited output power of electrical amplifier, it cannot provide high enough power for RF signal. Therefore, the phase relationship of the electrical signals on PM1 and PM2 should be carefully adjusted to generate more peaks with flat amplitude. Here, the RF signals entering PM1 and PM2 can be given as $Vd1(t) = R_1 V_\pi \sin(2\pi f_s t)$ and $Vd2(t) = R_2 V_\pi \sin(2\pi f_s t + \Delta\varphi)$ respectively [24], where $\Delta\varphi$ is the phase shift of the $Vd1(t)$ and $Vd2(t)$.

The output optical signal of PM2 is expressed as

$$E_{PM2} = E_{cw} \exp(j\pi R_1 \sin(2\pi f_s t)) \times \exp(j\pi R_2 \sin(2\pi f_s t + \Delta\varphi))$$
$$= E_{cw} \exp\{j\pi[R_1 \sin(2\pi f_s t) + R_2 \sin(2\pi f_s t + \Delta\varphi)]\}$$
$$= E_{cw} \exp[j\pi R_c \sin(2\pi f_s + \Phi)] \tag{5}$$

From Eq. (5), we can find out that the two driven RF signals drive the cascaded PM1 and PM2, which have the same expression function. Therefore, we can combine PM1 and PM2 as one combined PM, where $Vd(t) = Vd1(t) + Vd2(t)$ and $\tan\Phi = R_2 \sin\Delta\varphi/(R_1 + R_2 \cos\Delta\varphi)$. Therefore, the modulation factor of the combined PM is given by

$$R_c = \sqrt{R_1{}^2 + 2R_1 R_2 \cos\Delta\varphi + R_2{}^2} \tag{6}$$

As we can see from Eq. (6), the modulation factor of the combined PM is determined by R_1, R_2 and phase shift $\Delta\varphi$. We can adjust the phase shift of the RF signals entering PM1 and PM2 with caution to attain more peaks with little changed amplitude. For simplicity, we get $\Delta\varphi = 0$ and $R_c = R_1 + R_2$.

In our approved scheme, we can get more flattened subcarriers from the cascaded PMs. For the cascaded PMs, the RF driven signal can be represented as $Vd(t) = R_c V_\pi \sin(2\pi f_s t)$. Then, the output lightwave of the optical frequency comb can be given as

$$E_{ofc}(t) \approx E_0 \sum_{n=-m}^{+m} J_n(\pi R_c) \exp[j2\pi(f_c + nf_s)t] \tag{7}$$

where $2m + 1$ is the number of the subcarriers, f_s is the subcarrier frequency interval. As a result, the lightwave output signal of the PM2 can be shown as the optical central carrier and serval subcarriers, as shown in Fig. 1(c) [28].

After being amplified by an EDFA-1, a WSS selects two desired comb lines.

$$E_{wss}(t) \approx E_0\{J_{n_1}(\pi R_c) \exp[j2\pi(f_c + n_1 f_s)t] + J_{n_2}(\pi R_c) \exp[j2\pi(f_c + n_2 f_s)t]\} \tag{8}$$

One optical tone emitted from a port as the optical LO for heterodyne to generate THz-wave signal with the optical frequency of $f_c + n_2 f_s$. An optical tone from the other port is injected into the push-pull MZM, which carries a 4-Gbaud QPSK-modulated baseband signal and 1-Gbaud 16QAM-modulated baseband signal, which is expressed as

$$E_{MZM}(t) \approx E_0 \cdot [I(t) + jQ(t)] \cdot J_{n_1}(\pi R_c) \exp[j2\pi(f_c + n_1 f_s)t] \tag{9}$$

where $I(t) + jQ(t)$ denotes the modulated baseband vector signal. Then after being amplified by the EDFA-2 and combined with the optical LO by the 3-dB coupler. And the lightwave output before the UTC-PD is shown in Fig. 1(d), which is expressed as

$$E_c(t) \approx \frac{E_0\{[I(t) + jQ(t)] \cdot J_{n_1}(\pi R_c) \exp[j2\pi(f_c + n_1 f_s)t] + j \cdot J_{n_2}(\pi R_c) \exp[j2\pi(f_c + n_2 f_s)t]\}}{\sqrt{2}} \tag{10}$$

Then, at the output of the UTC-PD, the beating of the modulated optical tone with the optical LO in the UTC-PD generates THz-wave signal, which can be expressed as

$$i_{PD}(t) = \quad \mu|E_c(t)|^2 = \mu(E_0 J_{n_1}(\pi R_c))^2 [I^2(t) + jQ^2(t)] + \mu(E_0 J_{n_2}(\pi R_c))^2$$
$$+ 2\mu E_0{}^2 J_{n_1}(\pi R_c) J_{n_2}(\pi R_c) I(t) \sin\{2\pi(n_1 - n_2)f_s t\}$$
$$+ 2\mu E_0{}^2 J_{n_1}(\pi R_c) J_{n_2}(\pi R_c) Q(t) \cos\{2\pi(n_1 - n_2)f_s t\} \tag{11}$$

where μ represents the PD responsivity, A/W, which is expressed as

$$\mu = \frac{e\eta}{hf} \tag{12}$$

(a) Optical spectrum after ECL.

(b) Optical spectrum after PM1.

(c) Optical spectrum after PM2.

(d) Optical spectrum before UTC-PD.
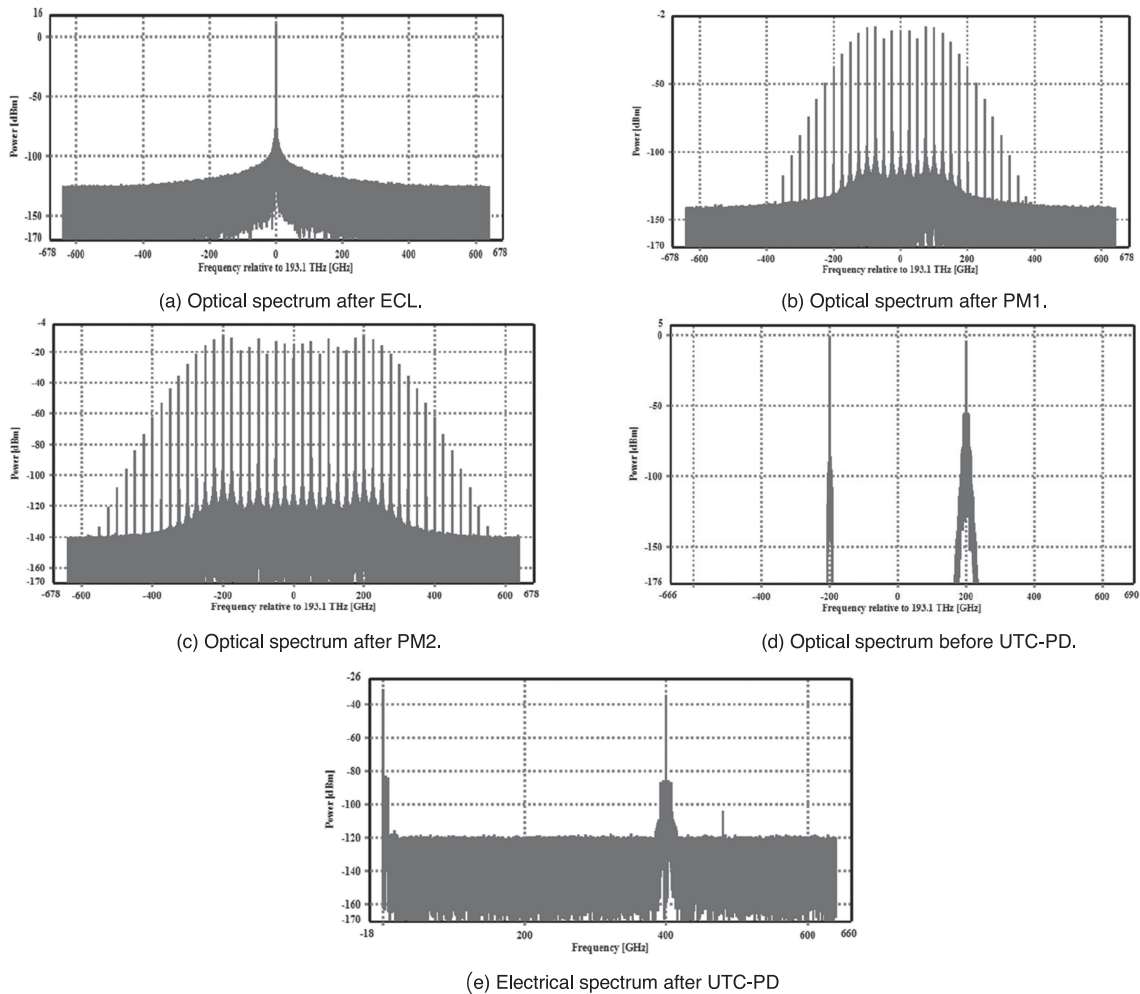

(e) Electrical spectrum after UTC-PD

Fig. 2. Optical spectra with a resolution of 0.01 nm.

where e represents electronic power, η denotes quantum efficiency, h denotes Planck's constant and f denotes the center frequency value of the optical carrier detected by UTC-PD.

As shown in Eq. (11), the first two terms of the current expression are direct current components, and the last term is the required THz-wave signal. n_1 and n_2 denote the two sidebands selected by WSS. Assuming $n_1 = 8$ and $n_2 = -8$, the 0.4 THz vector THz-wave signal generates.

3. Simulation Setup and Results

As depicted in Fig. 1, we built the simulation system on the basis of the simulation software VPI Photonics and study the photonic vector THz-wave generation based on optical frequency comb and single push–pull MZM. The CW lightwave at 193.1 THz emitted from one external cavity laser (ECL) with a mean output power of 15 dBm is modulated by the PM1 and PM2 in series with $V_\pi = 4V$, which are actuated by 25 GHz RF signal. And the ECL has a linewidth of around 100 kHz, as show in Fig. 2(a). We adjust the phase relation of the RF signals on PM1 and PM2 to extend the lightwave output of the optical frequency comb. Fig. 2(b) and Fig. 2(c) shows the simulated optical spectrum after PM1 and PM2, when $R_1 = R_2 = 2.8$, respectively. A total of 25 subcarriers are generated in the 600 GHz wavelength range centered at 193.1 THz. To ensure that the two
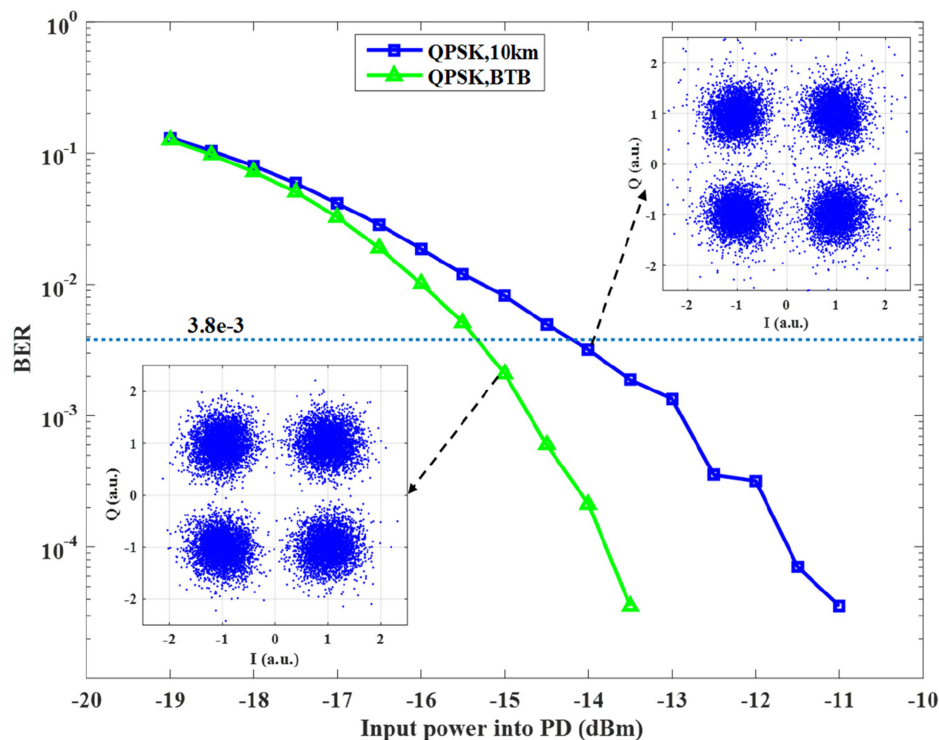
Fig. 3. BER versus the launched optical power into PD for 4-Gbaud QPSK.

optical frequency comb lines selected by WSS or interleave have large enough amplitude, we need to amplify the optical frequency comb to 5dBm by EDFA1. After passing through the WSS, the optical THz-wave signal is mainly made up of two optical comb lines with the frequency interval of 0.4 THz. As shown in Fig. 2(d), the joint spectrum after WSS is formed from one un-modulated LO tone at -8th-order sideband and the other optical tone with modulation at +8th-order sideband .The modulated optical tone is fed into the push-pull MZM, which carries a 4-Gbaud QPSK-modulated baseband data or a 1-Gbaud 16QAM-modulated baseband data in MATLAB. A pseudo-random binary sequence (PRBS) of one word length 2^{18}-1 maps the baseband QPSK signal or 16QAM signal.

The optical QPSK/16QAM signal is amplified to 5 dBm by EDFA2 before combining with the optical LO branch. After being amplified to be amplified to 5 dBm by the EDFA3, the combined lightwaves is injected into SSMF with attention coefficient of 0.18 dB/km, chromatic dispersion (CD) of 16.5 ps/nm/km, dispersion of slope of 0.075 ps/km/nm^2, and PMD coefficient of 0.5 ps/km$^{1/2}$.

At the receiver end, after passing through a variable optical attenuator (VOA), the received THz-wave signal is converted by a UTC-PD with sensitivity of 1 A/W, thermal noise of 10^{-18} W/Hz, including Gaussian shot noise. The two optical carriers of the optical THz-wave signal beat with each other and generate the 0.4 THz electrical THz-wave bearing the QPSK /16QAM signal, as shown the RF spectrum in Fig. 2(e). For the THz-wave signal, we utilize a mixer, driven by a sinusoidal LO source, to implement analog down conversion to intermediate frequency signal. Eventually, we can recovery the transmitter data from DSP, including down conversion to baseband, dispersion compensation, constant modulus algorithm (CMA) equalization for QPSK and cascaded multi-modulus algorithm (CMMA) equalization for 16QAM, frequency offset estimation, phase offset estimation and BER calculation [29].

BER versus the launched optical power into UTC-PD is shown in Fig. 3, when we use 0.4 THz THz-wave to transmit the 4-Gbaud QPSK-modulated transmitter signal over BTB and 10-km SSMF.
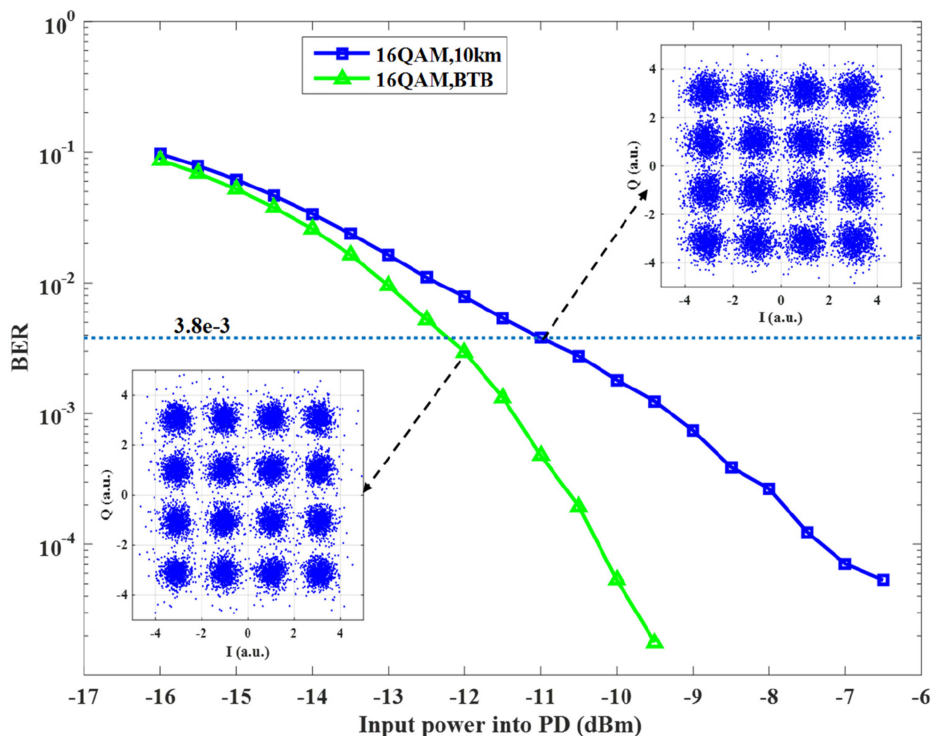
Fig. 4. BER versus the input optical power into PD for 1-Gbaud 16QAM.

As we can see from Fig. 3, while the input power into UTC-PD is greater than -15.5 dBm for BTB and -14 dBm for 10-km transmission, respectively, the BER is under the HD-FEC threshold of 3.8e-3. Due to the influence of the dispersion of the fiber, the constellation points of 10 km SMF-28 transmission case are more divergent than the constellation points of BTB case.

Fig. 4 shows the BER versus the launched optical power into UTC-PD, when we use 0.4 THz THz-wave to deliver the 1-Gbaud 16QAM-modulated transmitter signal over BTB and 10-km SSMF transmission. From Fig. 4, when the input power into UTC-PD is greater than -12 dBm for BTB and -10.8 dBm for 10-km transmission, respectively, the BER is under the HD-FEC threshold of 3.8e-3. Due to the influence of the dispersion of the fiber, the constellation points of 10 km SMF-28 transmission case are more divergent than the constellation points of BTB case. The simulation results strongly support our theoretical results.

4. Conclusion

A novel photonic vector THz-wave generation on the strength of optical frequency comb and single push-pull MZM is demonstrated with simulation software VPI Photonics. We use cascaded PM1 and PM2 to generate optical frequency comb and extend the spectrum for the generation of high frequency THz-wave signal. The simulated results validate that the transmission performance of the QPSK-modulated signal and 16QAM-modulated signal is desired and the BER can be less than the FEC threshold of 3.8e-3. As we know, this is the first report to achieve the generation of the THz-wave based on optical frequency comb and single push-pull MZM. This work offers the support for the further investigation of high-frequency THz generation. With the performance improvement of related devices that restrict terahertz technology, terahertz optical communication technology will be greatly developed.

References

[1] T. Kleine-Ostmann and T. Nagatsuma, "A review on Terahertz communications research," *J. Infrared, Millimeter Terahertz Waves*, vol. 32, no. 2, pp. 143–171, 2011, doi: 10.1007/s10762-010-9758-1.

[2] H. Song and T. Nagatsuma, "Present and future of Terahertz communications," *IEEE Terahertz Sci. Technol.*, vol. 1, no. 1, pp. 256–263, Sep. 2011, doi: 10.1109/TTHZ.2011.2159552.

[3] A. J. Seeds, H. Shams, M. J. Fice, and C.C. Renaud, "TeraHertz photonics for wireless communications," *J. Lightw. Technol.*, vol. 33, no. 3, pp. 579–587, Feb. 2015, doi: 10.1109/JLT.2014.2355137.

[4] P. T. Dat, A. Kanno, T. Umezawa, N. Yamamoto, and T. Kawanishi, "Millimeter- and terahertz-wave radio-over-fiber for 5G and beyond," in *Proc. IEEE Photon. Soc. Summer Topical Meeting Series*, 2017, pp. 165–166.

[5] X. Li *et al.*, "120 Gb/s wireless Terahertz-Wave signal delivery by 375 GHz-500 GHz Multi-Carrier in a 2 × 2 MIMO system," *J. Lightw. Technol.*, vol. 37, no. 2, pp. 606–611, Jan. 2019, doi: 10.1109/JLT.2018.2862356.

[6] L. Gonzalez-Guerrero *et al.*, "Comparison of optical single sideband techniques for THz-Over-Fiber systems," *IEEE Terahertz Sci. Technol.*, vol. 9, no. 1, pp. 98–105, Jan. 2019, doi: 10.1109/TTHZ.2018.2884736.

[7] K. Liu *et al.*, "100 Gbit/s THz photonic wireless transmission in the 350-GHz band with extended reach," *IEEE Photon. Tech. Lett.*, vol. 30, no. 11, pp. 1064–1067, Jun. 2018, doi: 10.1109/LPT.2018.2830342.

[8] S. Jia *et al.*, "120 Gb/s Multi-Channel THz wireless transmission and THz receiver performance analysis," *IEEE Photon. Tech. Lett.*, vol. 29, no. 3, pp. 310–313, Feb. 2017, doi: 10.1109/LPT.2016.2647280.

[9] A. Stohr, M. F. Hermelo, M. Steeg, P. B. Shih, and A. Ng'Oma, "Coherent radio-over-fiber THz communication link for high data-rate 59 Gbit/s 64-QAM-OFDM and real-time HDTV transmission," in *Proc. Opt. Fiber Commun. Conf. Exhib.*, 2017, pp. 1–3.

[10] H. Shams *et al.*, "100 Gb/s multicarrier THz wireless transmission system with high frequency stability based on A Gain-Switched laser comb source," *IEEE Photon. J.*, vol. 7, no. 3, pp. 1–11, Jun. 2015, doi: 10.1109/JPHOT.2015.2438437.

[11] S. Koenig *et al.*, "Wireless sub-THz communication system with high data rate," *Nat. Photon.*, vol. 7, no. 12, pp. 977–981, 2013, doi: 10.1038/nphoton.2013.275.

[12] J. Ma, "Dual-Tone QPSK optical Millimeter-Wave signal generation by frequency nonupling the RF signal without phase precoding," *IEEE Photon. J.*, vol. 8, no. 4, pp. 1–7, Aug. 2016, doi: 10.1109/JPHOT.2016.2585351.

[13] C. Wang, J. Yu, X. Li, P. Gou, and W. Zhou, "Fiber-THz-Fiber link for THz signal transmission," *IEEE Photon. J.*, vol. 10, no. 2, pp. 1–6, Apr. 2018, doi: 10.1109/JPHOT.2018.2809433.

[14] C. Wang, J. Yu, X. Li, P. Gou, and W. Zhou, "Fiber-THz-Fiber link for THz signal transmission," *IEEE Photon. Photon. J.*, vol. 10, no. 2, pp. 1–6, Apr. 2018, doi: 10.1109/JPHOT.2018.2809433.

[15] H. Shams, *et al.*, "100 Gb/s multicarrier THz wireless transmission system with high frequency stability based on A Gain-Switched laser comb source," *IEEE Photon. Photon. J.*, vol. 7, no. 3, pp. 1–11, Jun. 2015, doi: 10.1109/JPHOT.2015.2438437.

[16] Z. Li *et al.*, "SSBI mitigation and the Kramers–Kronig scheme in Single-Sideband Direct-Detection transmission with Receiver-Based electronic dispersion compensation," *J. Lightw. Technol.*, vol. 35, no. 10, pp. 1887–1893, May 2017, doi: 10.1109/JLT.2017.2684298.

[17] G. Ducournau *et al.*, "Ultrawide-Bandwidth Single-Channel 0.4-THz wireless link combining broadband Quasi-Optic photomixer and coherent detection," *IEEE Terahertz Sci. Technol.*, vol. 4, no. 3, pp. 328–337, May 2014, doi: 10.1109/TTHZ.2014.2309006.

[18] X. Yu *et al.*, "160 Gbit/s photonics wireless transmission in the 300-500 GHz band," *APL Photon.*, vol. 1, no. 8, p. 81301, 2016, doi: 10.1063/1.4960136.

[19] T. Nagatsuma, G. Ducournau, and C.C. Renaud, "Advances in terahertz communications accelerated by photonics," *Nat. Photon.*, vol. 10, no. 6, pp. 371–379, 2016, doi: 10.1038/nphoton.2016.65.

[20] X. Yu *et al.*, 60 Gbit/s 400 GHz wireless transmission, in *Proc. IEEE Int. Conf. Photon. Switching*, 2015, pp. 4–6.

[21] S. Jia *et al.*, "120 Gb/s Multi-Channel THz wireless transmission and THz receiver performance analysis," *IEEE Photon. Technol. Lett.*, vol. 29, no. 3, pp. 310–313, Feb. 2017, doi: 10.1109/LPT.2016.2647280.

[22] H. Shams *et al.*, "Optical frequency tuning for coherent THz wireless signals," *J. Lightw. Technol.*, vol. 36, no. 19, pp. 4664–4670, Oct. 2018, doi: 10.1109/JLT.2018.2846031.

[23] T. Shao *et al.*, "Phase noise investigation of multicarrier Sub-THz wireless transmission system based on an injection-locked gain-switched laser," *IEEE Terahertz. Sci. Technol.*, vol. 5, no. 4, pp. 590–597, Jul. 2015, doi: 10.1109/TTHZ.2015.2418996.

[24] J. Zhang *et al.*, "Generation of coherent and frequency-lock multi-carriers using cascaded phase modulators and recirculating frequency shifter for Tb/s optical communication," *Opt. Express.*, vol. 19, no. 14, pp. 12891–12902, 2011, doi: 10.1364/OE.19.012891.

[25] T. Ishibashi, Y. Muramoto, T. Yoshimatsu, and H. Ito, "Unitraveling-Carrier photodiodes for Terahertz applications," *IEEE J. Sel. Top. Quantum*, vol. 20, no. 6, pp. 79–88, Nov./Dec. 2014, doi: 10.1109/JSTQE.2014.2336537.

[26] Y. Li *et al.*, "Characterization of Sub-THz Photonic-Transmitters based on GaAs–AlGaAs uni-traveling-carrier photo-diodes and substrate-removed broadband antennas for impulse-radio communication," *IEEE Photon. Technol. Lett.*, vol. 20, no. 16, pp. 1342–1344, Aug. 2008, doi: 10.1109/LPT.2008.926855.

[27] X. Pan *et al.*, "Photonic vector mm-wave signal generation by optical dual-SSB modulation and a single push-pull MZM," *Opt. Lett.*, vol. 44, no. 14, p. 3570, 2019, doi: 10.1364/OL.44.003570.

[28] L. Zhao, L. Xiong, M. Liao, S. Liu, and X. Yu, "QPSK vector Millimeter-Wave signal generation based on odd times of frequency without precoding," *IEEE Photon. J.*, vol. 10, no. 6, pp. 1–9, Dec. 2018, doi: 10.1109/JPHOT.2018.2878873.

[29] X. Li *et al.*, "QAM vector signal generation by optical carrier suppression and precoding techniques," *IEEE Photon. Technol. Lett.*, vol. 27, no. 18, pp. 1977–1980, Sep. 2015, doi: 10.1109/LPT.2015.2448517.